AUT Journal of Civil Engineering

AUT J. Civil Eng., 2(1) (2018) 49-58
DOI: 10.22060/ajce.2018.12560.5257

Parametric Study on Confined Masonry Walls Subjected to In-plane Cyclic Loading Through Numerical Modeling

B. Shakarami, M.Z. Kabir*, R. Sistaninejad

Department of Civil and Environmental Engineering, Amirkabir University of Technology, Tehran, Iran

ABSTRACT: Results of numerical study on confined masonry walls are described in this paper, which presents a discussion on the behavior of confined masonry walls with different aspect and reinforcement ratio subjected to the in-plane horizontal loads, using advanced numerical simulations in LS-DYNA environment. A non-linear finite element micro-model based on smeared crack and total strain-stress models is used to examine existing tested masonry walls. The masonry units include solid clay bricks and concrete blocks, the mortar and bonding interfaces between the units and mortar have been lumped in continuum elements. In order to validate micro-modeling strategy the input data is based on a combined confined wall which was previously tested in the literature with a clearly identification and justification. The numerical results are presented as force-displacement curves, types of failure modes, ductility and energy absorption. It was observed that the confined walls with an aspect ratio of (h/l=1) shows better performance in terms of resisting mechanism, deformability and energy absorption.

Review History:

Received: 4 April 2017
Revised: 20 January 2018
Accepted: 10 March 2018
Available Online: 1 April 2018

Keywords:
Confined Masonry Wall
FE Modeling
In-plane Response
Cyclic Loading
Ductility
Energy Absorption

1- Introduction

Nowadays the confined masonry is a dominant method of construction in many countries [1]. Confined masonry walls are usually made of clay bricks or concrete blocks restrained with reinforced concrete tie-columns and bond-beams. Confined masonry is a dominant method of construction for housing. In fact, confined masonry is also widely used for housing in most countries like Iran. Walls represent the main resisting structural element in masonry buildings ensuring resistance not only to vertical loading but also to the lateral loading, in earthquake prone areas. Recent earthquakes have shown that unreinforced or non-confined masonry systems, even if not so old, do not behave adequately for seismic loading, exhibiting brittle response and damage [2]. This behavior is mainly attributed to the low strength of un-reinforced masonry walls under tensile stresses induced by lateral loading, by insufficient robustness of the units and poor connection between floors and walls. The primary distributed reinforcement or confining elements improves significantly the seismic performance of masonry elements, leading to higher lateral resistance and ductility [3, 4].

Two methods of numerical analysis are widely used for modeling of masonry constructions: macro and micro-modeling. In macro-modeling approach, there is no difference between brick units and mortar and a homogenization approach uses to obtain the mechanical characteristics of new material. In fact, the analysis of masonry structures with large number of units and joints can only be carried out with macro-models, in which a relation between average stresses and strains in the composite material is established. In micro modeling method, both brick units and mortar joints are considered separately in numerical modeling and an interface element is taken to model discontinuity of masonry constituents. The benefit of using this approach is that all the different failure mechanisms such as potential crack, slip or crushing planes and composite interface model, which includes a tension cut-off for mode I failure and Colomb friction envelope for mode II failure can be considered. But the fact that little importance has been given to the numerical modeling of masonry is confirmed by the absence of well-established micro-model [5, 6].

Numerical modeling of masonry structures can effectively be useful for better understanding of masonry wall's mechanical behavior. This powerful tool can help the researchers to predict the behavior of masonry walls tested at a laboratory [7]. In the case of confined masonry, the available knowledge is adequate. Testing is expensive and takes time but is the best way to provide the strength, the capacity to dissipate energy and the failure modes of non-conventional practice. Still, less expensive and less time consuming alternatives for testing need to be used, if not to replace them, at least to complement them. For this purpose, a series of confined masonry walls

Corresponding author, E-mail: mzkabir@aut.ac.ir

examined under in-plane cyclic loads are considered for numerical study. The wall configurations are studied with different aspect ratio and reinforcement. An overview of the numerical result with details is given first. Finally, the quality of the numerical results is assessed.

2- Description of experimrntal test in literature

In the first step, it is intending to validate the proposed numerical modeling in this study with the experimental result of the combined confined masonry specimen tested under in-plane loading. For this purpose, the presented test setup shown in Figure 1 is implemented. The further detailed parameters are available in [8]. The wall with the dimensions of 190 cm × 200 cm is a combination of concrete blocks and clay bricks which are surrounded by horizontal and vertical concrete members. The confining tie-column and bond beam members are 120 mm× 120 mm × 200 mm concrete elements with a compressive strength of 14.7 MPa. Four #3 longitudinal bars with diameters of 3/8" and (F_Y=412 Mpa) are used for beam and columns and transversal reinforcement involves #2 bars (1/4" in diameter) each 20 cm and (F_Y=216 Mpa). The typical clay brick and concrete blocks dimensions are 23 cm × 12 cm × 5.5 cm and 38 cm × 12 cm × 18.5 cm, respectively. The wall geometrical characteristics and reinforcement bars in the study were selected to be close to the previously tested confined brick walls [7, 8]

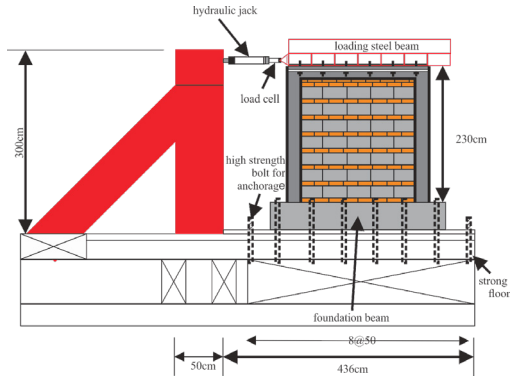

Figure 1. Experimental setup of tested wall [8]

3- Numerical Modeling

The micro-model of the tested walls is shown in Figure 2. 8-nodes plane stress continuum elements are used for the masonry units and 6-nodes interface elements are adopted for the masonry joints. In the case of units, iso-parametric elements with Gaussian quadrature scheme were adopted, [9, 10], as shown in Figure 3. Potential vertical cracks of the units were applied at mid-length of the units. The joints were lumped into the brick units and the Unit-mortar interface was modeled by an interface element (6-node elements), see Figure 3. The Newton-Raphson iteration is considered by using displacement control procedure and an energy convergence criterion is used as an appropriate tolerance. As in the case of experimental test, cyclic horizontal displacement is applied at the mid-height of concrete beam on the top of the wall.

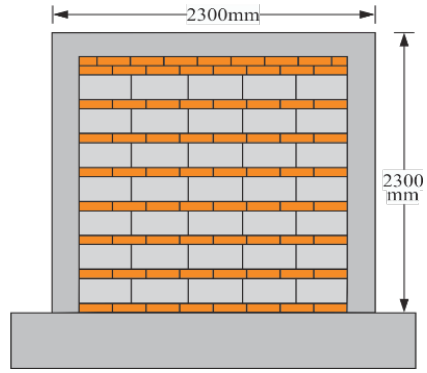

(a) wall dimensions

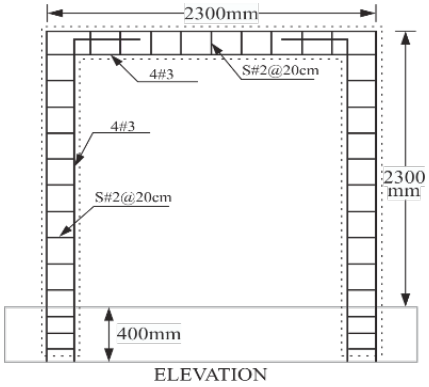

(b) reinforcement detail

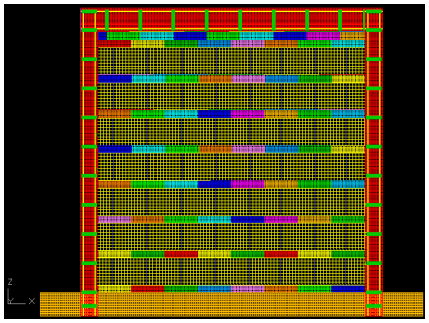

(c) LS-DYNA modeling

Figure 2. Micro model of combine-confined wall

Figure 4 shows the comparison between in-plane loading versus in-plane displacement diagram of the numerical modeling in LS-DYNA environment. The results show a reasonable agreement between two graphs. It should be noted that all basic failure modes of masonry walls can be considered in the micro-modeling approach used in this study. Micro-modeling method enables the detailed illustration of masonry behavior as failure mechanisms and also strength and displacement capacity; therefore several authors used this type of simulation to evaluate masonry elements response [11-13]. In the following sections, a parametric study is performed on masonry walls with different aspect ratios by changing masonry unit size and different bond-beam and tie-column dimensions. In-plane cyclic loading is considered for investigated specimens.

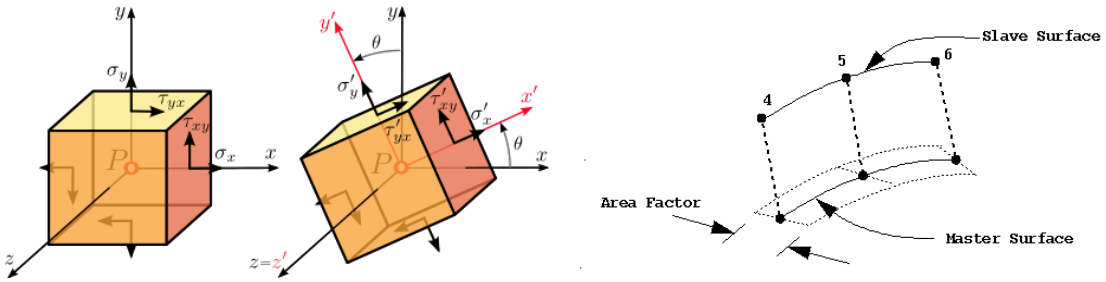

(a) Plane stress continuum element, (8-noded)

(b) interface element, (6-noded)

Figure 3. LS-DYNA elements used in numerical modeling [10]

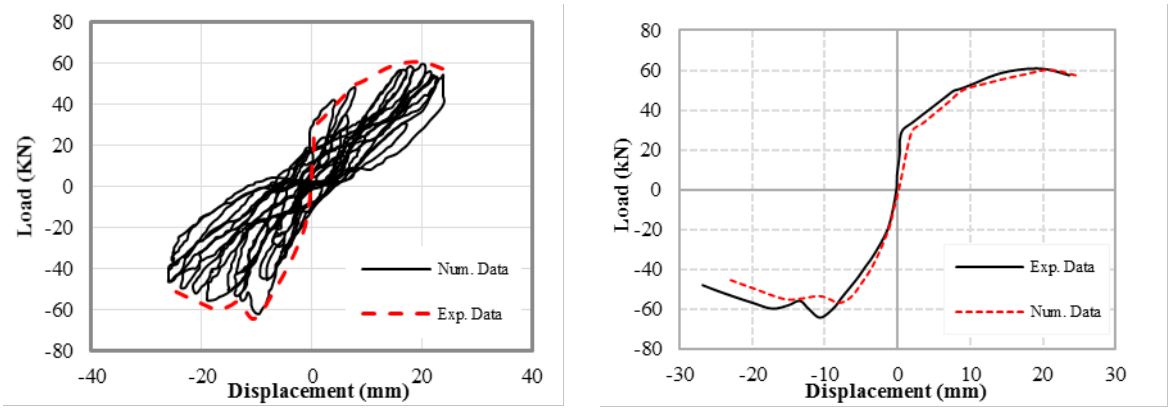

(a) Numerical hysteresis loop

(b) Experimental hysteresis loop of MCC-4 [8]

Figure 4. Comparison of experimental and numerical analysis of masonry wall under in-plane cyclic Loading

4- Geometrical Properties

Confined masonry walls with different parameters including: the wall dimensions, reinforcement ratio and bond-beam and tie-column size are studied in the parametric investigation, as presented in Table 1. Each specimen is characterized by three parts name. The first part is devoted to the shape of the walls; SQ, SL, and HR for Square, Slender and Horizontal walls, respectively. S and C in the second part represent solid bricks and concrete blocks and the number refer to the number of steel bars in confined elements. One of the confined wall specimens (SQS6) is depicted in Figure 5.

Table 1. Summary of numerical confined masonry walls models

Specimens	Dimension of wall(mm)	Brick type	Dimension (cm)		Reinforcement		
			beam	column	beam	column	Stirrup
*SQS4	1000×100×1000	Solid brick	25×25	20×20	4Φ10	8Φ10	Φ6@20(cm)
SQS6	1000×100×1000	Solid brick	25×25	20×20	6Φ12	12Φ12	Φ6@20(cm)
**SLS4	1000×100×2000	Solid brick	25×25	20×20	4Φ10	8Φ10	Φ6@20(cm)
SLS6	1000×100×2000	Solid brick	25×25	20×20	6Φ12	12Φ12	Φ6@20(cm)
***HRS4	2000×100×1000	Solid brick	25×25	20×20	4Φ10	8Φ10	Φ6@20(cm)
HRS6	2000×100×1000	Solid brick	25×25	20×20	6Φ12	12Φ12	Φ6@20(cm)
SQCB4	1000×300×1000	Concrete.B	30×25	15×20	4Φ10	8Φ10	Φ6@20(cm)
SLCB4	1000×300×2000	Concrete.B	30×25	15×20	4Φ10	8Φ10	Φ6@20(cm)
HRCB4	2000×300×1000	Concrete.B	30×25	15×20	4Φ10	8Φ10	Φ6@20(cm)

*SQ=Square, **SL=Slender, ***HR=Horizontal Rectangle, C=Confine, B= Block, CB= Concrete Block

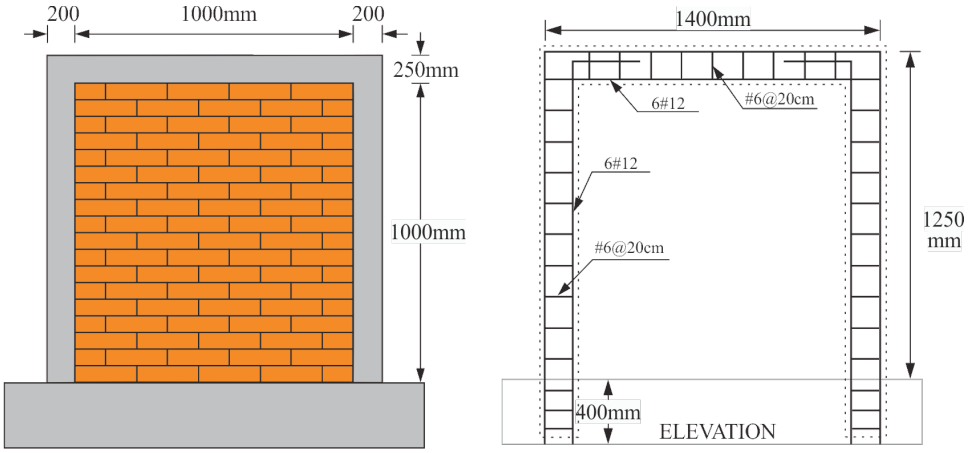

Figure 5. Dimension of confined wall, (SQS6)

5- Loading and Boundary Condition

In this study, the specimens are subjected to the in-plane cyclic loading. The compressive axial load, as gravitational load, is applied at the first step and is kept constant. Horizontal displacement is consequently applied on the top of the walls until failure. Normalized axial stress equal to σ/f_a =0.1 and σ/f_a = 0.2 are considered in the parametric analysis for fixed end walls, respectively, where σ is the pre-compression load applied to the wall and fa is the compressive strength of masonry. For the specimens with unit aspect ratio and normalized axial stresses mentioned above, the shear failure is the dominant mode of failure based on results of Arturo [8], so the effect of confined elements can be apparent in the failure mode and response of masonry walls. Regarding the boundary condition when considered as an integrant part of a structural masonry building, masonry walls tend to behave with top and bottom boundaries mostly fixed, meaning that the restriction is effective on both ends. Continuum elements representing the masonry units located at the base of the wall are connected to the interface elements which are fully fixed in order to simulate fixed base conditions for the masonry walls. The upper beam is connected to the wall through interface elements modeled with linear behavior and infinite stiffness to simulate a perfect bond between connected elements.

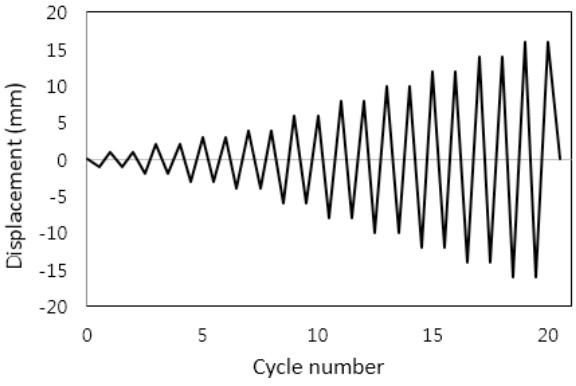

Figure 6. Cyclic testing protocol used, Arturo [8]

6- Material Model and Mechanical Property

In the micro modeling approach, all constituent material of the concrete block and solid brick masonry walls as distinct mechanical properties are independently described. Distinct materials are used to represent the behavior of concrete part, masonry units, vertical and horizontal joints and the potential cracks in the middle of the units. The mechanical properties used in the description of the material models are obtained from an experimental test carried out on materials and masonry assemblage [8, 14, 15]. A three-dimensional cohesive interface model is used for modeling of interfaces in this paper. This model is based on smooth yield surface reduces the computation time and restricts the failure of corners [16, 17]. Also, LS-DYNA has fully automated contact analysis capability, which makes this software very user-friendly for contact analysis problems [18]. All mechanical parameters used for numerical modeling are shown in Tables 2-5. According to Lorenco, it is useful to model potential cracks in units in order to avoid over-estimation of the collapse load and stiffness. Therefore, potential cracks are placed at the middle length of units and modeled with interface elements by discrete cracking model, Tables 3 and 4 [19]. The constitutive law for discrete cracking by LS-DYNA is based on total deformation theories which express the stresses as a function of the total relative displacement [18-20]. Normal and shear stiffness of potential cracks are considered as $K_n=10^6$ N/mm^3 and $K_s= 10^6$ N/mm^3, respectively [21].

Table 2. Properties for the potential brick cracks

k_n [N/mm^3]	k_s [N/mm^3]	F_t [N/mm^2]	G_f^1 [N/mm]
1×10^6	1×10^6	2.0	0.08

Table 3. Elastic properties for the bricks and joints

Brick		Joint	
E [N/mm^2]	υ	k_n [N/mm^3]	k_s [N/mm^3]
15270	0.2	31.90	17.07

Table 4. Inelastic properties for the joints

Tension		Shear				cap	
F_t [N/mm²]	G_f^1 [N/mm]	c [N/mm²]	tan ϕ	tanψ	G_f^2 [N/mm]	F_m	C_{ss}
0.36	0.018	1.4 Ft	0.75	0.0	0.47	15	9

Table 5. Mechanical properties of brick and concrete elements [8]

brick				Concrete block				Concrete elements
F_m [Mpa]	E[N/mm²]	F_r [Mpa]	υ	F_{mc}[Mpa]	E[N/mm²]	F_r [Mpa]	υ	F'_c [kg/cm²]
10.1	15270	0.86	0.2	4.2	15572	0.96	0.2	150

Table 6. Results of solid brick confined walls

Wall name	Elastic shear force [kN]	Maximum Strength [kN]	Δ_y [mm]	Δ_u [mm]	Ductility (μ_Δ)	Energy absorption [kN.mm]
SQS4	119.21	152.48	3.6	14.5	4.02	1601.124
SQS6	143.671	173.11	2.99	11.7	3.91	1628.422
SLS4	43.092	51.92	4.8	19.18	3.90	809.429
SLS6	44.231	63.87	4.92	15.93	3.23	819.921
HRS4	96.22	124.4	3.5	13.8	3.94	1592.017
HRS6	99.73	146.11	3.5	13.67	3.90	1598.01

7- Parametric Study

Parametric analysis is performed for assessment of the influence of different parameters on the lateral behavior of confined masonry walls. Numerical simulation is considered to evaluate the in-plane response of confined walls consist of solid clay bricks and concrete blocks with different aspect ratios. In addition, reinforcement ratio in confining elements is changed. Obtained results are presented in following sections.

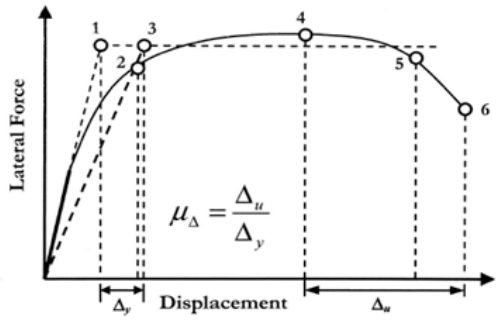

Figure 7. Procedure of calculating ductility

7- 1- Ductility and energy absorption

Ductility is a measure of inelastic deformations such as displacement, curvature and strain. It is defined as the ratio of maximum to effective yield deformation (Figure 7). The most difficult part of defining ductility is devoted to determining when yield and ultimate deformations occur [22]. The displacement ductility is defined as:

$$\mu_\delta = \delta_u / \delta_y \quad (1)$$

Where μ_δ is displacement ductility, δ_u is ultimate displacement at 80% of ultimate load and δ_y is yield displacement of elastoplastic approximation. The yield displacement is defined as the yield force of elastoplastic approximation to the initial secant stiffness.

In addition, the total energy absorption by each wall specimen is calculated at the end of the displacement level in which failure occurred for the positive loading direction. The total energy is calculated as the area under the hysteresis loops, using the Trapezoid Rule. The total dissipated energy is defined by Equation 2:

$$E = \sum (\delta_{i+1} - \delta_i)(F_{i+1} + F_i)/2 \quad (2)$$

Where F is the force and is displacement.

7- 2- Numerical results of walls with solid clay bricks

Numerical results of the examined walls with solid clay bricks are presented in this section. The square walls with the aspect ratio of one (h/l=1), failed under shear as shown in Figure 8a. In these walls, cracks created at the upper half of the wall and extended with increasing of the lateral displacement. On the other hand in walls with an aspect

ratio of two (h/l=2), failure occurs under flexure. Horizontal flexural cracks appeared at the first joint from the bottom due to increasing of tensile stresses associated to the flexure of the wall, see Figure 8b. Also in walls with an aspect ratio of 0.5 (h/l=0.5), sliding shear cracks started from the bottom of the wall and propagated with increasing lateral displacement increment (see Figure 8c).

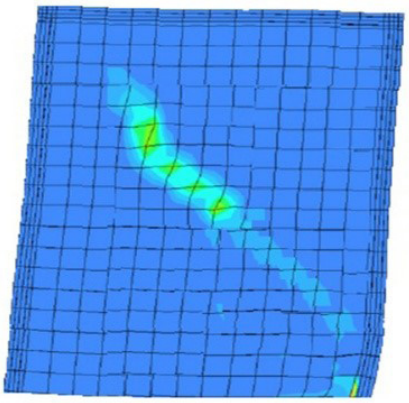

(a)diagonal shear failure (SQC4)

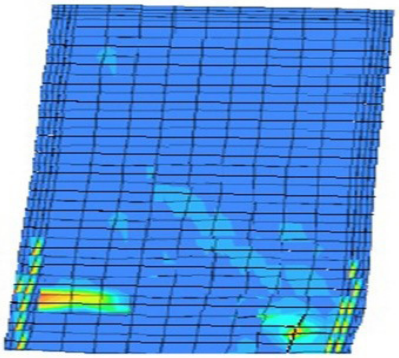

(b)flexural failure (SLS6)

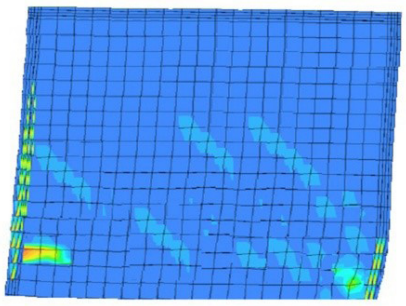

(c)sliding shear failure (HRS4)

Figure 8. Typical configuration of failure mode of masonry walls (principal stresses)

Summary of numerical results in terms of elastic shear force, peak strength, yield and ultimate displacements, ductility, and energy absorption are compared in Table 6. The maximum strength of square walls is more than other walls as expected. The ductility values of examined specimens are approximately identical as shown in Table 6.

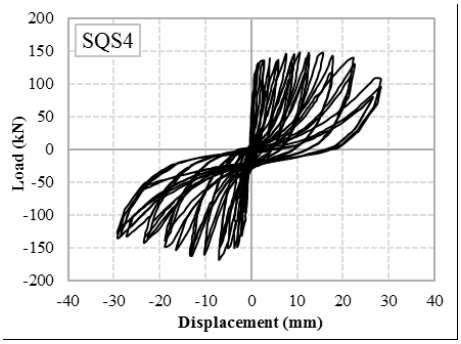

(a) SQS4

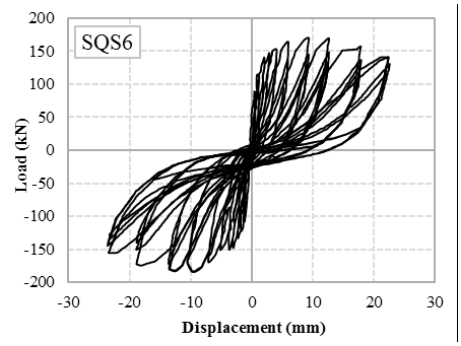

(b) SQS6

Figure 9. Hysteretic load-displacement curves of square specimens under cyclic lateral displacement and 2 N/mm² vertical compressions

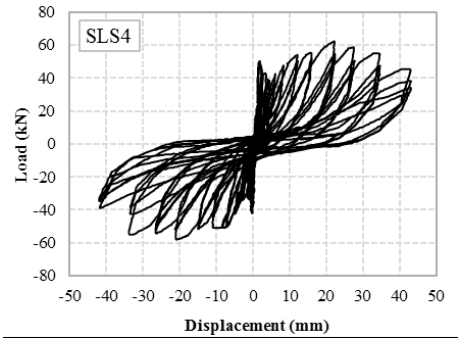

(a) SLS4

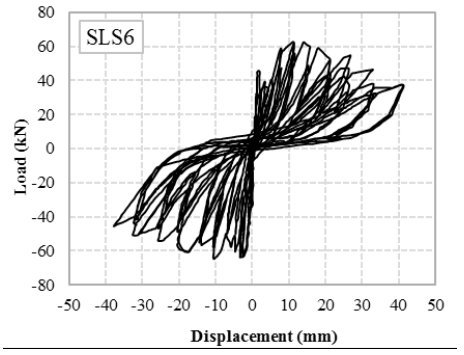

(b) SLS6

Figure 10. Hysteretic load-displacement curves of slender specimens under cyclic lateral displacement and 2 N/mm² vertical compressions

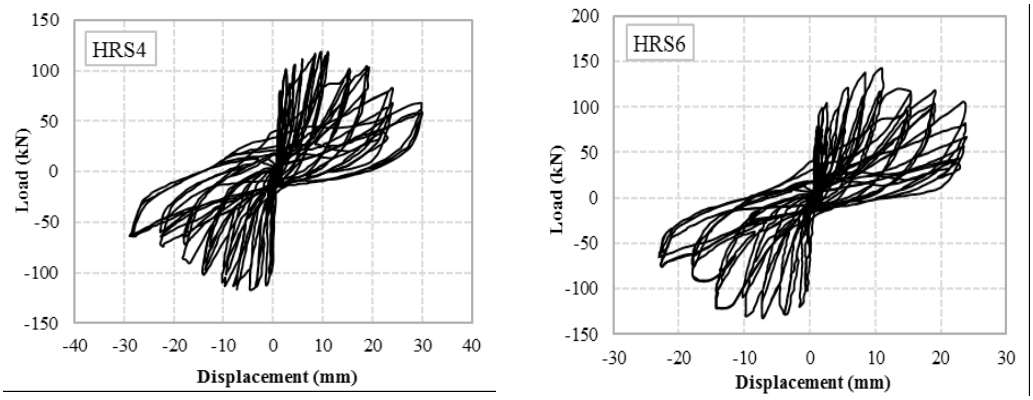

(a) HRS4 (b) HRS6

Figure 11. Hysteretic load-displacement curves of horizontal specimens under cyclic lateral displacement and 2 N/mm² vertical compressions

The load-displacement hysteresis curves of the wall specimens made of clay solid bricks are presented in Figures 9 to 11. The walls with an aspect ratio of one (h/l=1), have the better condition in the case of lateral strength. Comparison of the specimens with the same geometrical dimension but different reinforcement ratio shows that increasing the steel bars number in confining elements resulted in a stiffness gain in square walls, but this increment is not observed in slender walls with an aspect ratio of two (h/l=2). Regarding the stress at the brick-mortar interface, results show a uniform distribution of shear stress in bricks and vertical mortar joints in masonry walls which failed in flexure. In the walls which failed in shear, a decrease in shear stresses of vertical mortar joints and an increase in shear stress of bricks are observed.

By comparing SQ specimens, it is obvious that shear strength of wall SQS6 is more than the other three walls. The ultimate load of the walls SQS4 and SQS6 are around 152.48 kN and 173.11 kN respectively (Figure 9b). In addition, wall SQS6 had more energy absorption rather than SQS4 due to more reinforcement ratio. Yield and ultimate displacements are required for calculating of ductility values. The values of δy and δu are computed as described in the literature [Priestley]. The maximum an elastic force of SQS4 is 119.2 kN and occurs at 3.6 mm displacement while in SQS6 wall, elastic load of 143.67 is occurred at a displacement of 2.99 mm. SQS4 is more ductile rather than SQS6 (Figure 9).

Results show the similar confining effect on the crack pattern of both square walls. The shear cracks of SQS4 and SQS6 mostly developed in the upper half of the wall and diagonal crack mechanism is observed and compression struts are formed. In addition, for both models crack started at the upper left corner of the wall and the bricks are separated mostly between mortars towards the lower right corner. The crack pattern of square specimens is shown in Figure 8a. It must be noted that the walls with an aspect ratio of 0.5 (h/l=0.5), have a similar condition as the walls with the aspect ratio of one (h/l=1). Considering the results of slender specimens, wall SLS6 is resisted against more lateral loads and ultimate strength is approximately 63.87 kN, while the maximum load of the wall SLS4 is around 51.92 kN as can be concluded from Figures 10a and 10b. More energy is dissipated by SLS6 that SLS4 as observed in square walls. In the case of ductility, maximum elastic forces are 43.092 kN and 44.231 kN and corresponding displacements are 0.85 and 0.9 for SLS4 and SLS6 respectively. The maximum displacement occurred at 3.3mm in wall SLS4 and 3.51 in wall SLS6, so ductility ratio in SLS4 is more ductile than SLS6. The governing failure mode of slender specimens is a flexural failure as shown in Figure 8b and cracks are started at the upper left corner. In addition, bricks separated mostly between mortars and this failure propagated through lower right corner. The load-displacement hysteresis curves for wall specimens HRS4 and HRS6 are presented in Figure 11. Results of the walls HRS4 and HRS6 that are presented in Figure 11 show that the wall HRS6 has better condition in the case of maximum strength. The lateral strength of the wall HRS6 is 17.5% more that the wall HRS4. Maximum elastic force, yield displacement and ultimate displacement of the wall HRS4 are 96.22 kN, 3.5 mm and 13.8 mm respectively. These values are 99.73 kN, 3.5 mm and 13.67 mm for the wall HRS6. The dominant failure mode of HR walls is sliding shear as shown in Figure 8c. Shear cracks happen the lower part of the wall HRS4 and HRS6. In Figure 12, pushover envelope curves of confined walls with solid clay bricks are shown.

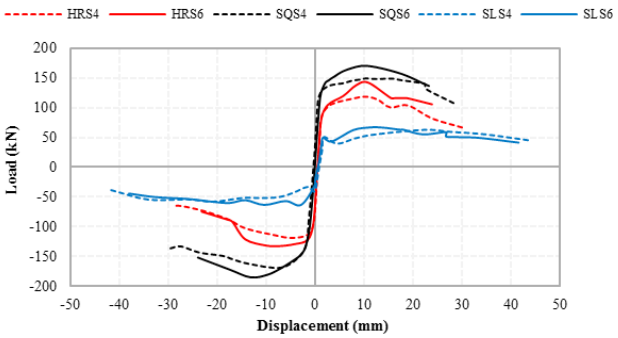

Figure 12. Comparison of pushover envelope curves for solid clay brick walls

7- 3- Numerical results of walls with concrete blocks

Numerical results of the walls with concrete block units are presented in Table 7. As observed in solid clay brick walls, the ultimate strength of the square wall is more than the other two walls. Yield displacement and ultimate displacement of SLC4 is considerably higher than SQC4 and HRC4.

The load-displacement hysteresis curves of the walls made of concrete block units are presented in Figures 13 and 14. Envelope of each curve is illustrated in Figure 15.

In the examined models of this section, SQC4 resisted against more lateral loads. The ultimate shear load of the specimen is 154.11 kN, while the capacity of the other two specimens reached to 73.82 kN for SLC4 and 117.83 kN for HRC4. The maximum elastic force of each wall that corresponds to the yield displacement is 147.28 kN, 85.5 kN and 101.2 kN for the walls SQC4, SLC4, and HRC4 respectively. Corresponding displacements are reported in Table 7.

Crack patterns of the walls SQC4, SLC4 and HRC4 governed by horizontal flexural cracking at the heel of the walls spread at low levels of horizontal displacement. With increasing lateral displacements, diagonal cracks suddenly developed at specimen SQC4; also sliding shear crack occurred at bottom of the wall HRC4, with localized cracks (Figure 16). The diagonal crack in the squat specimen propagated through units and mortar without a preferential path. This behavior is consistent with a good connection between two materials that indicates a reasonably homogenous material. The results of both clay brick and concrete block walls show that square walls have more energy absorption rather than slender and horizontal walls because of the failure mechanism and profitable mechanism of load transform. Horizontal walls are in the next place with energy absorption near to the squat walls. The slender specimens that their failure governed by flexure, absorbed energy less than the other walls. The values of dissipated energy and ductility ratio are compared for all walls in Figure 17. In this figure, the difference between ductility and energy absorption of the walls with the same aspect ratio but different masonry unit type and various reinforcement ratio is presented.

Table 7. Results of concrete block walls

Wall name	Elastic shear force [kN]	Maximum Strength [kN]	Δ_y [mm]	Δ_u [mm]	Ductility (μ_Δ)	Energy absorption [kN.mm]
SQC4	147.28	154.111	2.98	12.02	4.026	1600.924
SLC4	85.5	73.82	5.6	22	3.92	977.112
HRC4	101.2	117.826	3.5	13.9	3.97	1582.411

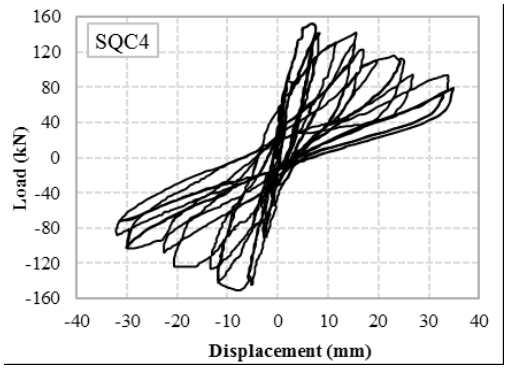

(a) SQC4

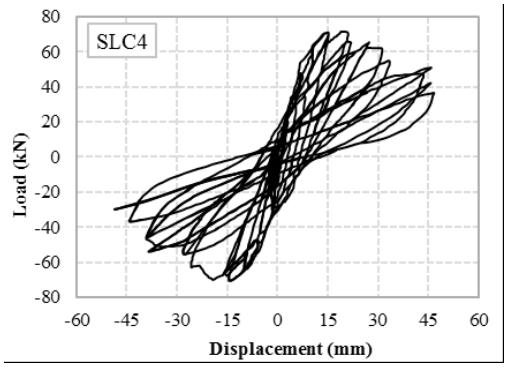

(b) SLC4

Figure 13. Hysteretic load-displacement curves of square and slender specimens made of concrete block units

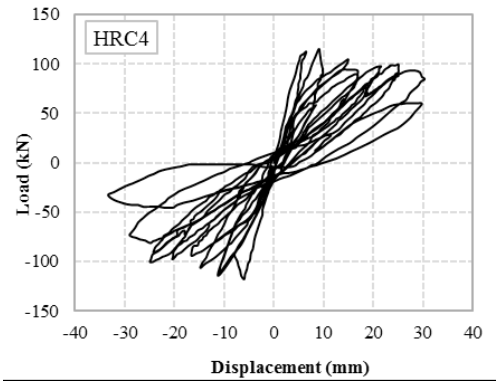

Figure 14. Hysteretic load-displacement curve of wall HRC4

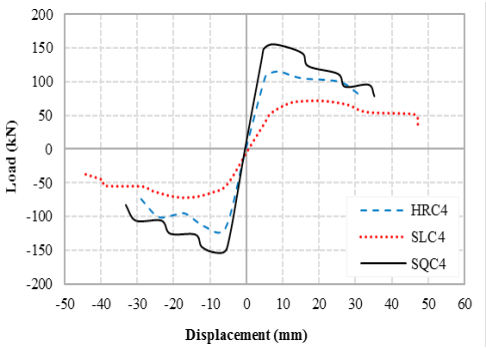

Figure 15. Comparison of pushover envelope curves for concrete block walls

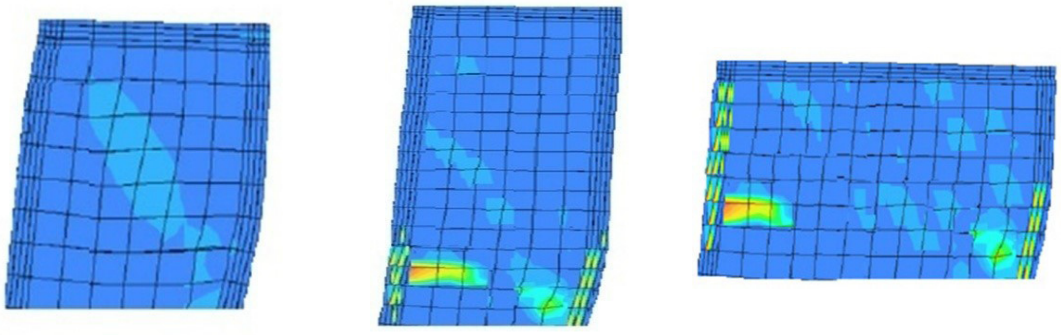

(a) shear failure mode of SQC4 (b) flexural failure mode of SLC4 (c) sliding shear failure mode of HRC4

Figure 16. Failure modes of confined concrete block walls (principal stresses)

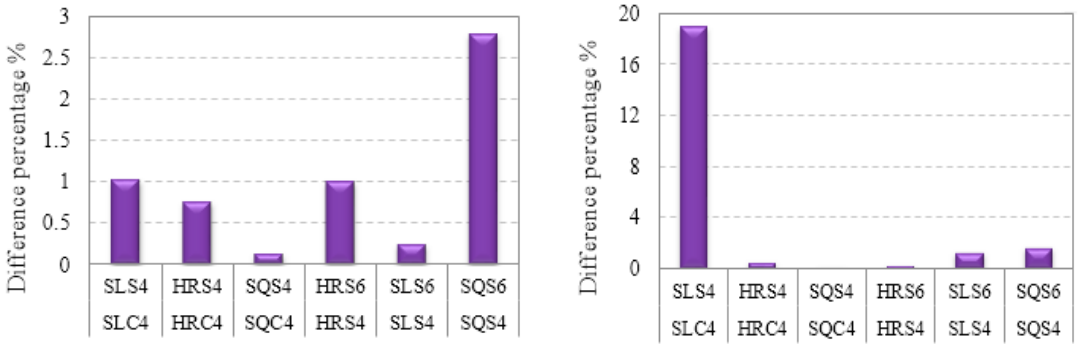

(a) ductility (b) energy absorption

Figure 17. Percentage of difference between confined masonry walls with different aspect ratio

In the examined models of this section, SQC4 resisted against more lateral loads. The ultimate shear load of the specimen is 154.11 kN, while the capacity of the other two specimens reached to 73.82 kN for SLC4 and 117.83 kN for HRC4. The maximum elastic force of each wall that corresponds to the yield displacement is 147.28 kN, 85.5 kN and 101.2 kN for the walls SQC4, SLC4, and HRC4 respectively. Corresponding displacements are reported in Table 7.

Crack patterns of the walls SQC4, SLC4 and HRC4 governed by horizontal flexural cracking at the heel of the walls spread at low levels of horizontal displacement. With increasing lateral displacements, diagonal cracks suddenly developed at specimen SQC4; also sliding shear crack occurred at bottom of the wall HRC4, with localized cracks (Figure 16). The diagonal crack in the squat specimen propagated through units and mortar without a preferential path. This behavior is consistent with a good connection between two materials that indicates a reasonably homogenous material. The results of both clay brick and concrete block walls show that square walls have more energy absorption rather than slender and horizontal walls because of the failure mechanism and profitable mechanism of load transform. Horizontal walls are in the next place with energy absorption near to the squat walls. The slender specimens that their failure governed by flexure, absorbed energy less than the other walls. The values of dissipated energy and ductility ratio are compared for all walls in Figure 17. In this figure, the difference between ductility and energy absorption of the walls with the same aspect ratio but different masonry unit type and various reinforcement ratio is presented.

As shown in Figure 17a, in square walls with an aspect ratio of 1 and slender walls with an aspect ratio of 0.5, ductility shows higher difference percentage. In addition, due to similar reinforcement and cross-sectional area of confining elements, minimum difference is observed for the walls SQS4 and SQC4. By comparing energy absorption of Figure 17b, the difference percentage between walls SQS4 and SQC4 is minimizing again. The maximum difference is recorded for SLS4 and SLC4.

8- Conclusion and final remarks

This paper deals with the numerical investigation of confined masonry wall system based on concrete blocks and solid clay bricks masonry units, to be used in low to medium rise residential buildings in seismic areas. A general overview of the main results of numerical study is provided and a detailed description of numerical modelling is also given. The input parameters for the material models have been determined from experimental test and from guidelines available in the literature. Two different masonry units: solid clay bricks and concrete blocks are examined in the modeling approach. The main following conclusion can be drawn:

1. Steel bars in confined elements increased the stiffness and lateral strength of masonry walls subjected to horizontal loading.
2. Considerable ductility is obtained because of confining elements.

3. The behavior of the walls with an aspect ratio of one (h/l=1) is better than the other walls in terms of shear strength and energy absorption.
4. Shear cracks are mostly observed at confined walls with aspect ratio of one (h/l=1), while confined walls with aspect ratio of two (h/l=2) failed by flexural cracks. Rocking failure mode is also achieved for walls with ratio of 0.5 (h/l=0.5).

There is a substantial difference between square and other types of confined walls in the case of energy absorption. The comparison of ductility between confined walls whether with clay bricks or concrete blocks represents a close relation. Indeed there is a correlation between concrete elements (tie-column and bond-beam) and reinforcement. In addition, the maximum strength increased with reduction of aspect ratio.
It is noteworthy to mention that this paper did not present practical design implication and results pointed out some aspects of confined masonry walls behavior.

References

[1] R. Meli, Structural Design Of Masonry Building, ACI special publication 147 masonry in the America, American concrete institute, (1994) 239-262.

[2] Klinger. R., Behavior of Masonry in the Northridge (Us) And Tecoman – Colima (Mexico) Earthquakes: Lessons Learned, And Changes in Us Design Provisions, Construction building material, 20(4) (2006) 209-219.

[3] N.J. Shing PB, Klamerus E, Spaeh H, Inelastic Behavior Of Concrete Masonry Shear Walls, Journal of structural engineering, 115(9) (1989) 2204-2225.

[4] T.e. M., Earthquake-Resistant Design of Masonry Buildings., Innovations in structures and construction. London: Imperial College Press, (1999).

[5] J.G.R.a.J.B.J. P. B. Lourenco, Continuum Model for Masonry: Parameter Estimation and Validation. Journal of structural engineering, 124(6) (1998) 642-652.

[6] P.B.Lourenco, V. G. Haach, Parametric Study of Masonry Walls Subjected to In-Plane Loading through Numerical Modeling, Engineering Structure, 3(4) (2011) 1377-1389.

[7] M.M.A. K. Chaimoon, Modeling of Confined Masonry Walls under Shear and Compression. Engineering Structure, 29(3) (2007) 2056-2068.

[8] J.A.A.a.H.S.V. T. C. Arturo, Cyclic Behavior of Combined and Confined Masonry Walls, Engineering Structure, 31(240-59) (2009).

[9] L.P. Zucchini A, Validation of a Micro-Mechanical Homogenisation Model: Application to Shear Walls, International journal Solids Structure, 46(3-4) (2009) 871-886.

[10] J.O.a.B. Halquist, D.J., Ls – Dyna User's Manual ("Nonlinear Dynamic Analysis Of Solids In Three Dimension ", 3 ed., University of California, Lawrence, Livermore National laboratory, rept, UCID- 19156 1987.

[11] P.B.L. V. G. Haach, Parametric Study of Masonry Walls Subjected to In-Plane Loading through Numerical Modeling, Engineering Structure, 3(4) (2011) 1377-1389.

[12] A.B. J. M. Adam, T. G. Hughes and T. Jefferson, Micromodelling of Eccentrically Loaded Brickwork: Study of Masonry Wallettes, Engineering Structure, 32(5) (2010) 1244-1251.

[13] G. Mohamad, Mechanism Failure of Concrete Block Confined Masonry under Compression, University of Minho, Guimaraes, Portugal, 2007.

[14] V.G. Haach, Development Of A Design Method For Confined Masonry Subjected To In-Plane Loading Based On Experimental And Numerical Analysis, University of Minho, Guimaraes, Portugal, Portugal, 2009.

[15] R.J. Lourenco PB, Multisurface Interface Model for Analysis of Masonry Structures, Engineering Mechanic, 123(7) (1997) 660-668.

[16] L.P. Milani G, Tralli A, Homogenised Limit Analysis Of Masonry Walls. Part I: Failure Surfaces, Computer Structure, 84(3-4) (2006) 166-180.

[17] G.V. Zijl, Modeling Masonry Shear–Compression: Role of Dilatancy Highlighted, Engineering Mechanic, 30(11) (2004) 1289-1296.

[18] S. Bala, Tie-Break Contacts in Ls-Dyna. , USA, 2007.

[19] L. PB, Computational Strategies for Masonry Structures, Delft University of Technology, 1996.

[20] T. Bakeer, Collapse Analysis Of Masonry Structures Under Earthquake Actions, Dresden University of Technology, Publication Series of the Chair of Structural Design, Germany, 2009.

[21] L. PB, Computational Strategies for Reinforced Masonry Structures, Delft University of Technology, 1996.

[22] M.J.N.Priestly. a.M.J. Kowalsky, Direct Displacement-Based Design of Concrete Buildings, Bulletin of the New Zealand National Society for Earthquake Engineering, 33(4) (2005) 421-444.

Please cite this article using:
B. Shakarami, M.Z. Kabir, R. Sistaninejad, Parametric study on confined masonry walls subjected to in-plane cyclic loading through numerical modeling, *AUT J. Civil Eng*, 2(1) (2018) 49-58.
DOI: 10.22060/ajce.2018.12560.5257